Ibn Al-Haitham Journal for Pure and Applied Sciences
Journal homepage: jih.uobaghdad.edu.iq
PISSN: 1609-4042, EISSN: 2521-3407
IHJPAS. 2026; 39(1)

Synthesis, Optical Energy Gap and Gas Sensing Properties of TiO_2 Doped Cr_2O_3 Thin Films

Nihad K. Ali[1*] and Ikhlas H. Shallal[2]
[1,2]Department of Physics, College of Education for Pure Science /Ibn Al-Haitham, Baghdad University, Baghdad, Iraq
[*]Corresponding Author

Received: 22/July/2025.
Accepted:25/September/2025
Published: 20/January /2026.
doi.org/10.30526/39.1.4258

Abstract

Thin films of Titanium dioxide (TiO_2) doped Chromium oxide (Cr2O3) with a thickness of (200 ± 20) nm and a doping ratio of (0.2, 0.4, 0.6, 0.8)% employed on glass and n-type porous silicon substrates by using Pulsed laser ablation technique. A Cr2O3: TiO2/PSi heterojunction for a gas sensor device was synthesized with Nd: YAG laser with 1064nm wavelength with 500 pulses of laser energy 600mJ. The effect of the dopant concentration ratios on absorption coefficient, optical energy gap and gas sensing properties such as sensitivity, responsivity and recovery times in the presence of 400ppm concentration of H_2S gas, were studied and discussed. The doped samples showed increased absorption coefficient values with higher doping concentrations. The optical band gap ranged from 3.95 eV-3.71 eV for the pure and TiO2 doped Cr2O3 thin films. The optimum sensitivity was (166.24%) when the doping ratio of TiO2 was 0.6% when exposed to an H2S-reduced gas at an operating temperature of 100°C.

Keywords: Thin films, Optical, Gas sensing, Cr_2O_3:TiO_2, Laser ablation.

1. Introduction

Semiconductor metal oxides have garnered significant attention in various fields of materials science and chemistry due to their exceptional magnetic, optical, and electrical properties[1]. The most metal elements can form a large diversity of oxide compounds[2], multiple metal oxide semiconductors, the one that has attracted further attention is chromium oxide (Cr_2O_3) because of its diversity of functions in its nano scaled structure, Cr_2O_3 has a p-type semiconducting nature, overage oxygen, and high magnitude refractive index with wide optical bandgap energy (~3 eV) due to strong electronic delocalization is coupled with vibrations of the local environment, these properties made this kind of p-type metal oxide semiconductors good candidates for several applications as optical storage system and gas sensors[3,4]. In this field, titanium dioxide (TiO_2) has been the most favored material for gas sensor devices**,** due to its low resistivity [5, 6].

The typical behavior of gas sensors can be explained through key principles of gas detection mechanisms, including adsorption, chemical reactions, and changes in physical properties. For instance, in semiconductor gas sensors, gas molecules adsorb onto the sensor's surface, altering its electrical conductivity. This change is then measured to determine the concentration of the gas. Understanding these fundamental physical principles is essential for designing sensors that can perform optimally [7, 8]. In summary, an ideal gas sensor integrates high selectivity, sensitivity, quick response, stability, accuracy, reproducibility, linearity, low power consumption, robustness, cost-effectiveness, ease of calibration, and compact size for reliable and efficient gas detection In addition to Cr_2O_3 and TiO_2 metal oxides there are several kinds which were essential materials that could be important for gas sensing thin films such as NiO, V_2O_3, MoO_3, WO_3,

GeO_2, Co_3O_4, Fe_2O_3, Nd_2O_3, In_2O_3, Nb_2O_5, SrO, CuO, TiO2 and ZnO by estimating their resistance changing as a result of the adsorption of gas species on the thin film surface[9-13]. Porous silicon is the most wealthy and prosperous in the manufacturing of gas sensor devices. The interaction between surface area and gas molecules could cause an increase in selectivity for various gases and high sensitivity [14-16]. The optical energy gap magnitude (Eg) for pure and doped thin films Cr_2O_3 thin films on a glass substrate has been measured by using **Equation 1**[17]:

$$\alpha h\upsilon = Z[h\upsilon - E_g]^n \quad \textbf{(1)}$$

where (α) symbolizes the absorption coefficient, (hυ) indecates the photon′s energy (eV), (Z) is the constant and exponent n=0.5 for direct allowed transition, (Eg) represents the optical energy gap (eV). The sensor response (S%) for as-deposited thin films was measured by using **Equation 2**[18]:

$$\text{Sensitivity }\%(S) = \left(\frac{R_g - R_a}{R_a}\right) \times 100 \quad \textbf{(2)}$$

Where R_a and R_g are the thin film electrical resistance in air and in the presence of gas, respectively. Another gas sensor parameter is response time, which represents the time interval during which the sensor is exposed to the targeted gas and reaches 90% of the entire reading for the resistance variation. The recovery time signifies the time when the sensor resistance declines to 10% upon cessation of exposure to the gas.[19]

Hydrogen sulfide (H_2S) is a dangerous, colorless gas, and it is a corrosive, harmful, toxic, and sharp-smelling gas with a bad odor, fundamentally released by the production of biogas, purification of sewage, and the refineries of petrol[20-23]. For this reason, gas sensors with high sensitivity are manufactured to detect it.

Pulsed laser ablation in liquid (PLAL) is one of the important and common technique which is employed to synthesize nano-particles (NP_S) assembled in a form of high purity colloidal solution in short reaction time with absent of by-products and lack of necessity multistep procedures and vacuum, high temperature neither using explosive nor toxic chemical reactants, these properties make PLAL chemically clean, inexpensive, green and simple operation for industrial application of nano-particles[24].

This study investigates the effects of TiO_2-doped Cr_2O_3 thin films, deposited using ablated nanoparticles through the pulsed laser ablation technique, and examines their optical and gas sensing characteristics when exposed to reduced hydrogen sulfide (H_2S) gas.

2.Materials and Methods

Pulse laser ablation in liquid (PLAL) was employed to ablate the nano-particles (NP_S) of the chromium trioxide (Cr_2O_3) and titanium dioxide (TiO_2) , Firstly, A powders with purity of (99.999%) were provided by the companies (Sigma –Aldrich, China) and (Central Drug House, India) were scaled at 7g and 2g of Cr_2O_3 and TiO_2 respectively, and then, they were compressed under a pressure of 12 Tons via hydraulic compressed for 24 hours as a duration to make pellets with a diameter of 1.7cm, The pellet was localized at the base of a glass vessel with 20ml of deionized water also Nd:YAG pulsed laser type (Huafei) with 1064nm wavelength was used to radiate the pellets with 500 pulses of laser energy 600mJ, pulse frequency 8Hz, to focus the laser beam a 10cm focal length converging lens was used to make a laser spot on the target surface with a diameter of 2.3mm, a colloidal solution was synthesized after the ablation process continues with rotating the vessel, the pure and doped thin films with ratios (0.2, 0.4 , 0.6, 0.8)% of TiO_2 was deposited by drop-casting method on a glass and n-type porous silicon substrate with dimensions of $(1.5\times1.5)cm^2$ at 400℃, the effect of heating evaporates the liquid to form the thin films with thickness of (200 ± 20) nm which is determined by cross-section method using field emitting scanning electron microscopy (FE-SEM) type (TESCAN MIRA3, Czechia). Optical and sensitivity characteristics were identified for pure and doped Cr_2O_3 films with ratio (0.2, 0.4, 0.6, 0.8)% of TiO_2, UV-Vi Spectrophotometer (Lambda 365) from (Perkin Elmer) was used to investigate the optical properties of thin film were the wavelength range of optical

absorbance spectrum 300nm-1100nm was indicated at room temperature The measurements of gas-sensing which comprises thin film resistance variation in the presence of 400ppm concentration of H_2S gas, sensitivity, responsivity and recovery times of the samples were have discussed and calculated.

3.Results

3.1. Absorption Coefficient and Optical Energy Gap

The Absorption coefficient was calculated by the formula:

$$\alpha = 2.303 \frac{A}{t} \quad (3)$$

Where (A) and (t) are the optical absorbance and the thin film thickness, respectively [25].

Figure 1 gives the variation of the optical absorption coefficient as a function of wavelength with a thickness of (200 ± 20) nm and a concentration ratio of (0.2, 0.4, 0.6, 0.8)% deposited on a glass substrate at room temperature. It could be concluded that all prepared films exhibited high absorption coefficient values ($>10^4$ cm^{-1}) in the short-wavelength region, indicating that the absorption edge lies in the ultraviolet range. Additionally, the absorption coefficient values decreased with increasing wavelength. The doped samples showed increased absorption coefficient values with higher doping concentrations. The highest absorption coefficient value was recorded for the 0.6% TiO_2-doped sample, reaching 12.59×10^4 cm^{-1} at 302nm wavelength.

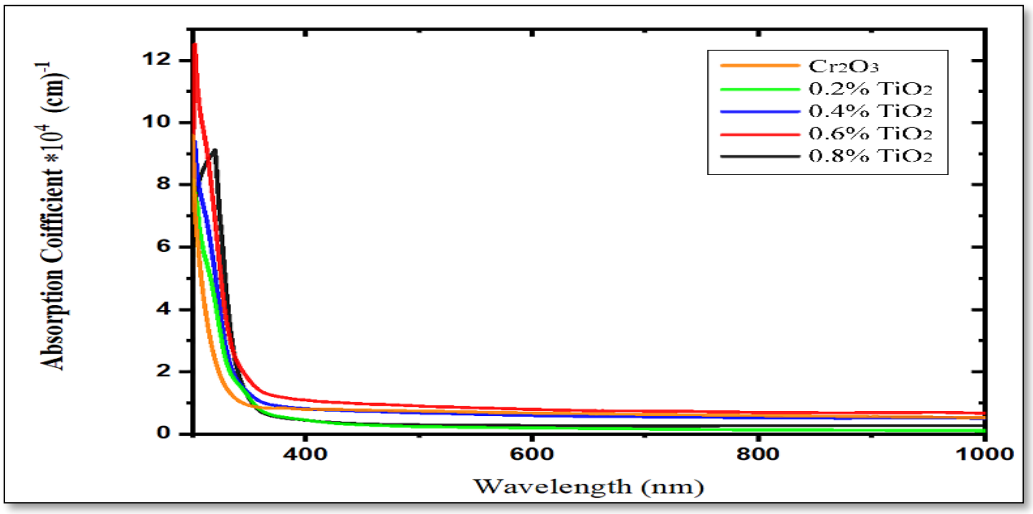

Figure 1. The optical absorption coefficient spectra for pure and TiO_2 doped Cr_2O_3 thin films.

The optical band gap energy of pure and doped Cr_2O_3 thin films, determined by Tauc's **Equation 1,** where n=0.5 for the allowed direct transition, when plotting $(\alpha h\nu)^2$ against the photon energy ($h\nu$) in x-axis, which clarifies that the energy band gap could be indicated by the intersection of the curve straight portion with the axis at α=0. **Figure 2** shows the energy gap, which was (3.95 eV) for pure Cr_2O_3 thin film. The energy gap was progressively decreased from (3.83 eV) at a concentration ratio of (0.2%) TiO_2 dopant, to (3.71 eV) at a concentration ratio of (0.8%) TiO_2 dopant. Consequently, a shift of the absorption spectrum to the visible domain was observed. The calculated values of the energy band gap are listed in **Table 1**.

Table 1. Optical band gaps (Eg)

Sample	Energy Gap (eV)
Cr_2O_3	3.95
Cr_2O_3: (0.2%)TiO_2	3.83
Cr_2O_3: (0.4%)TiO_2	3.75
Cr_2O_3: (0.6%)TiO_2	3.73
Cr_2O_3: (0.8%)TiO_2	3.71

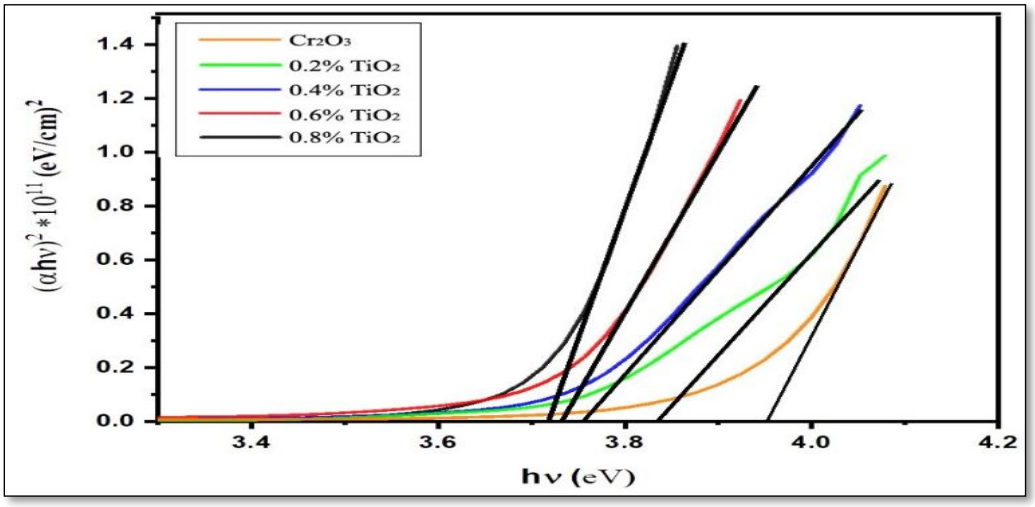

Figure 2. Optical energy gap for Cr_2O_3: TiO_2 thin films at different ratios of TiO_2.

3.2. Gas Sensor Characteristics

An ideal graph for a gas sensor illustrates the connection between the sensor's response (output signal) and the concentration of the target gas. A Cr_2O_3: TiO_2/PSi heterojunction for a gas sensor device was synthesized with a concentration ratio of TiO_2 dopant (0.2, 0.4, 0.6, 0.8) %. The sensor response was detected when exposed to 400 ppm of reduced hydrogen sulfide (H_2S) gas at various temperatures (25, 100, and 150) ℃. Thin film resistance was increased with time under reducing gas.

Figures 3 and **Table 2** illustrate that the sensitivity varied within the same sample as the operation temperature changed. Generally, sensitivity increased with a higher concentration ratio of TiO_2. The maximum sensitivity of 166.24% was recorded for the sample with a 0.6% TiO_2 ratio at 100°C, while a sensitivity of 120.67% was observed for the 0.4% TiO_2 sample at room temperature. In contrast, the 0.8% TiO_2 sample exhibited unusual behavior; it showed no sensitivity to H_2S gas at room temperature but demonstrated a high sensitivity of 103.49% at 150°C. Additionally, the response time increased in the samples with 0.2% and 0.4% TiO_2 but decreased in the 0.8% TiO_2 sample, which recorded the shortest response time of 9 seconds at both 100°C and 150°C. The 0.6% TiO_2-doped Cr_2O_3 thin film displayed enhanced sensitivity to hydrogen sulfide (H_2S) gas, making it an excellent candidate for gas sensing applications that aim to detect H_2S and monitor toxic gases in both environmental and industrial settings. Furthermore, the 0.8% TiO_2-doped sample had the shortest response time of 9 seconds. **Figure 4** summarizes the variation of sensitivity against H_2S gas at different ratios of TiO_2.

Table 2. The gas sensor properties

Sample	Operating Temp.(℃)	Sensitivity (%)	Response Time (s)	Recovery Time (s)
Cr_2O_3/PSi	R.T	30.57	14.4	75.6
	100	34.64	32.4	61.2
	150	37.86	17.1	52.2
Cr_2O_3:(0.2%)TiO_2/PSi	R.T	30.76	18	70.2
	100	27.08	25.2	63
	150	30.01	16.2	55.8
Cr_2O_3:(0.4%)TiO_2/PSi	R.T	120.67	23.4	90
	100	3.66	22.5	45.9
	150	2.04	24.3	45
Cr_2O_3:(0.6%) TiO_2/PSi	R.T	4.03	28.8	87.3
	100	166.24	20.7	89.1
	150	37.26	15.3	54
Cr_2O_3:(0.8%)TiO_2/PSi	100	87.88	9	78.3
	150	103.49	9	60.3
	200	33.87	16.2	52.2

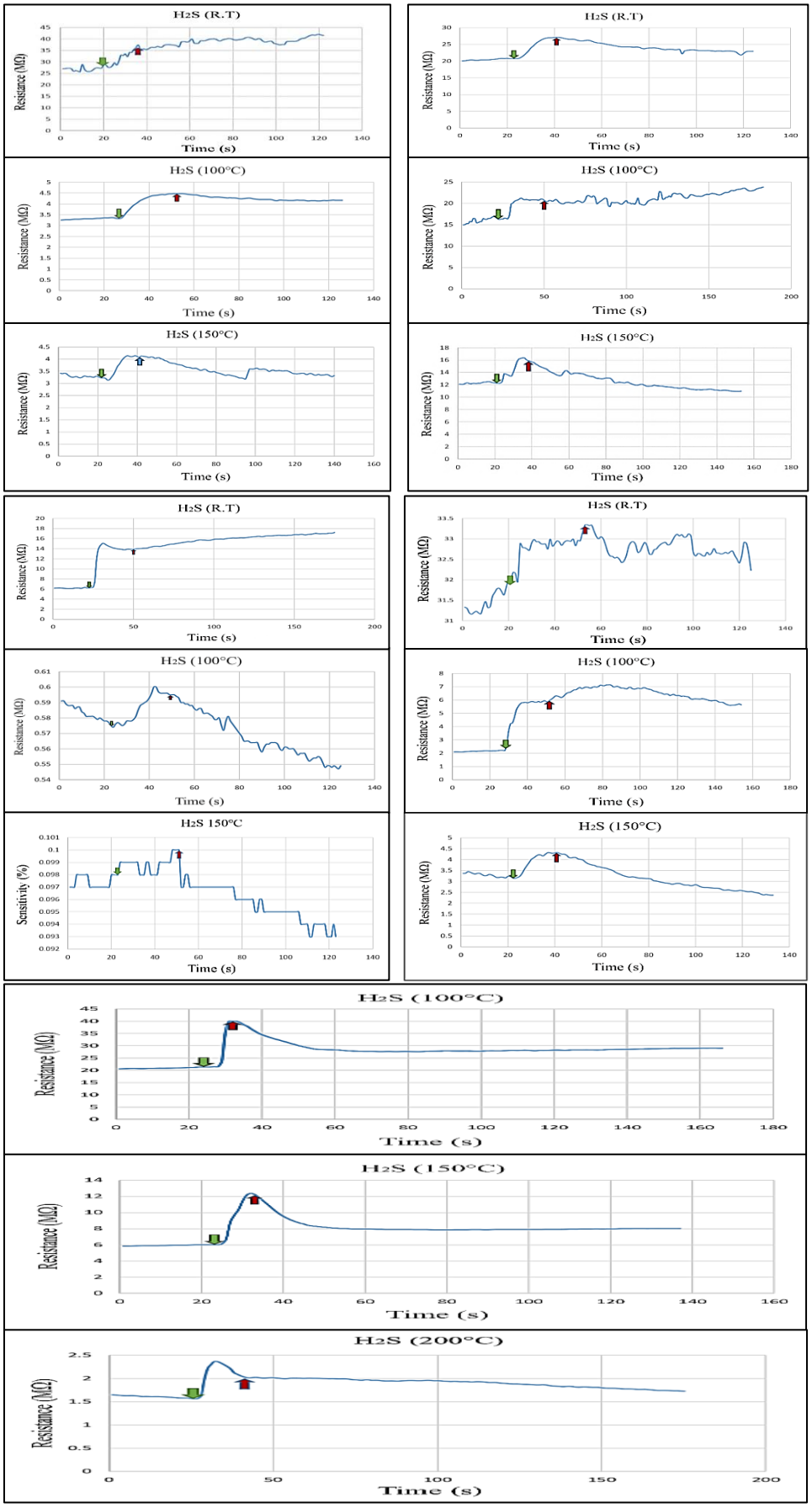

Figure 3. The variation of resistance as a function of time at different operation temperatures for Cr_2O_3: TiO_2/Psi heterojunctions with different doping ratios. a. Cr_2O_3 /Psi, b.Cr_2O_3:0.2% TiO_2/Psi, c.Cr_2O_3: 0.4% TiO_2/Psi, d.Cr_2O_3:0.6% TiO_2/Psi, e. Cr_2O_3:0.8% TiO_2/PSi

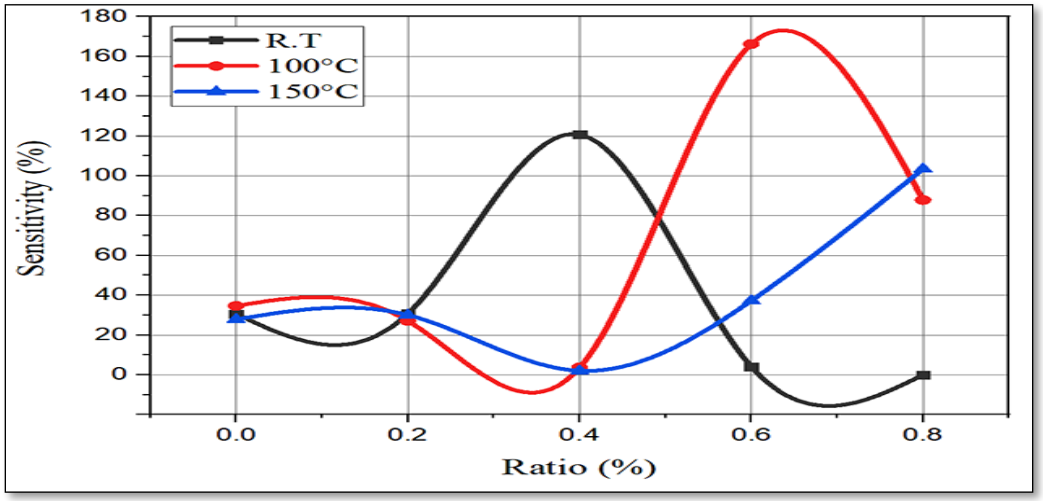

Figure 3. Variation of sensitivity against H_2S gas at a different ratio of TiO_2

4.Discussion

The results indicate the importance of doping by TiO_2 in enhancing the Cr_2O_3 thin films optical and gas sensor properties, the UV-Vis spectrometer findings showed a decrease in optical energy gap this result is in good agreement with many studies reported abroad for optical band gaps of thin films prepared by different techniques[26, 27], this decrease can be attributed to the incorporation of small amounts of TiO_2, with Cr_2O_3, leads to a re-arrangement of valence and conduction band energy levels, thereby reducing the value of band gap[28, 29]. High absorption coefficients has been observed in UV region of electromagnetic waves, which agrees with the study[5], make these films particularly suitable for optoelectronic applications requiring strong UV absorption[30].

The gas sensor findings reveals that all thin film showed an increase in resistance when exposed to the target gas which was ideal acting for a p-type semiconductor, where the electrons from the oxygen ion adsorption process were returned to the valence band, and then the recombination operation with the holes happened, it would cause a reduction in holes then the resistance is increased as a result of decreasing the conductivity[31]. The high sensitivity at different operation temperatures might be caused by the heterojunction's synergistic effect when the gas molecules react with the junction materials[32].

5.Conclusion

In conclusion, pure Cr_2O_3 and TiO_2-doped Cr_2O_3 nanostructures were produced using effective, simple, and cost-effective methods, specifically pulsed laser ablation in liquid (PLAL) and drop-casting techniques. Under these conditions, all samples exhibited a direct transition in their optical energy band gap. The pure chromium thin film had a band gap of 3.95 eV, which decreased to 3.71 eV with a 0.8% TiO_2 doping ratio. The Cr_2O_3:(0.6)TiO_2/Psi heterojunctions demonstrated increased sensitivity, achieving a response of 166.24% when exposed to hydrogen sulfide (H_2S) gas at an operating temperature of 100°C. This makes it an excellent candidate for gas sensing applications aimed at detecting H_2S and other toxic gases in both environmental and industrial settings. Additionally, the sample doped with 0.8% TiO_2 recorded the shortest response time, which was just 9 seconds.

Acknowledgment

This research would not be possible without the assistance of the Physics Department Staff, Deanship of the College of Education for Pure Science (Ibn Al-Haitham). I thank them wholeheartedly.

Conflict of Interest

The authors declare that they have no conflicts of interest.

Funding

None.

Ethical Clearance

The project was approved by the local ethical committee at the University of Baghdad.

References

1. Abdul Kareem SM, Jassim IK, Suhail MH. Cr2O3: TiO2 nanostructure thin film prepared by pulsed laser deposition technique as NO2 gas sensor. Baghdad Sci J. 2020;17(1 Suppl March):329-35. https://dx.doi.org/10.21123/bsj.2020.17.1(Suppl.).0329
2. Hassan TB, Mohammed GH. FTIR and optical properties of NiO doped Cr2O3 nanoparticles synthesis by hydrothermal method. Al-Mustansiriyah J Sci. 2018;29(1):168-73. http://doi.org/10.23851/mjs.v29i1.278
3. Suhail MH, Adehmash IK, Abdul Kareem SM, Tahir DA, Abdullah OG. Construction of Cr2O3:ZnO nanostructured thin film prepared by pulsed laser deposition technique for NO2 gas sensor. Trans Electr Electron Mater. 2020. https://doi.org/10.1007/s42341-020-00182-3
4. Singh J, Verma V, Kumar R, Kumar R. Structural, optical and electrical characterization of epitaxial Cr2O3 thin film deposited by PLD. Mater Res Express. 2019. https://doi.org/10.1088/2053-1591/ab3543
5. Salman SH, Shihab AA, Elttayef AK. Design and construction of nanostructure TiO2 thin film gas sensor prepared by R.F magnetron sputtering technique. Energy Procedia. 2019;157:283-9. https://doi.org/10.1016/j.egypro.2018.11.192
6. Liang Y, Ding M, Yang Y, Xu K, Luo X, Yu T, Liang Y, Ding M, Yang Y, Xu K, Luo X, Yu T, Zhang, W., Liu W. & Yuan C.. Highly dispersed Pt nanoparticles on hierarchical titania nanoflowers with {010} facets for gas sensing and photocatalysis. J Mater Sci. 2019;54:6826-40. https://doi.org/10.1007/s10853-019-03379-x
7. Salman SH, Hassan NA, Ahmed GS. Copper telluride thin films for gas sensing applications. Chalcogenide Lett. 2022;19(2):125-30. https://doi.org/10.15251/CL.2022.192.125
8. Abbas IA, Hazaa SQ, Salman SH. Employment of titanium dioxide thin film on NO2 gas sensing. J Phys Conf Ser. 2021;1879(3):032061. https://doi.org/10.1088/1742-6596/1879/3/032061
9. Alrazak AHA, Salman SH, Abbas IA, Mustafa MH, Ali HM, Abbas SA. Influence of doping with silver nanoparticles on the molybdenum trioxide gas sensor prepared by spray pyrolysis. Dig J Nanomater Biostruct. 2025;20(1):191-9. https://doi.org/10.15251/DJNB.2025.201.191
10. Abdul Kareem I, Oleiwi HF. Enhancing gas sensing performance of TiO2-ZnO nanostructures: effect of ZnO concentration. Ibn Al-Haitham J Pure Appl Sci. 2023;36(4):137-46. https://doi.org/10.30526/36.4.3173
11. Song Z, Yan J. Unveiling the doping effect of sub-4 nm ultrathin SnO2 quantum wires on gas sensors. Chem Mater. 2023;35(18):7750-60. https://doi.org/10.1021/acs.chemmater.3c01609
12. Wang L, Yao X, Yuan S , Gao Y., Zhang R, Yu X , Tu ST and Chen S. Ultra-high performance humidity sensor enabled by a self-assembled CuO/Ti3C2TX MXene. RSC Adv. 2023;13(9):6264-73. https://doi.org/10.1039/D2RA06903B
13. Hermawan A ,Zhang B ,Taufik A ,Asakura Y ,Hasegawa T,Zhu J ,Shi P and Yin S CuO nanoparticles/Ti3C2Tx mxene hybrid nanocomposites for detection of toluene gas. ACS Appl Nano Mater. 2020;3(5):4755-66. https://doi.org/10.1021/acsanm.0c00749
14. Salman SH, Jahil SS, Hassan NA, Abbas SA, Jasim KA. Ammonia gas sensing using porous silicon. J Phys Conf Ser. 2024;2857(1):012051. https://doi.org/10.1088/1742-6596/2857/1/012051
15. Dawood NS, Zayer MQ, Jawad MF. Preparation and characteristics study of porous silicon for vacuum sensor application. Karbala Int J Mod Sci. 2022;8(1):11. https://doi.org/10.33640/2405-609X.3209

16. Hadi HA, Ismail RA, Almashhadani NJ. Preparation and characteristics study of polystyrene/porous silicon photodetector prepared by electrochemical etching. J Inorg Organomet Polym Mater. 2019;29:1100-10. https://doi.org/10.1007/s10904-019-01072-9
17. Ibrahim FT, Abdughani SE. Effect of lasing energy on the structure and optical and gas sensing properties of chromium oxide thin films. Indian J Phys.2019. https://doi.org/10.1007/s12648-019-01492-w
18. Saruhan B, Lontio Fomekong R, Nahirniak S. Review: Influences of semiconductor metal oxide properties on gas sensing characteristics. Front Sens. 2021;2:657931. https://doi.org/10.3389/fsens.2021.657931
19. Pasupuleti K S. Pham TMT, Abraham B M, Thomas A M ,Vidyasagar D, Bak NH, Kampara R K, Yoon SG, Kim YH & Kim M D . Room temperature ultrasensitive ppb-level H2S SAW gas sensor based on hybrid CuO@V2C MXene van der Waals heterostructure. Adv Compos Hybrid Mater. 2025;8:132. https://doi.org/10.1007/s42114-024-01194-w
20. Wang H, Luo Y, Liu B, Gao L, Duan G. CuO nanoparticle loaded ZnO hierarchical heterostructure to boost H2S sensing with fast recovery. Sens Actuators B Chem. 2021;338:129806. https://doi.org/10.1016/j.snb.2021.129806
21. He H , Zhao C , Xu J, Qu K Jiang Z. Gao Z and Song YY. Exploiting free-standing p-CuO/n-TiO2 nanochannels as a flexible gas sensor with high sensitivity for H2S at room temperature. ACS Sens. 2021;6(9):3387-97. https://doi.org/10.1021/acssensors.1c01256
22. Zhang B, Shang F, Shi X, Yao R, Wei F, Hou X. Polyaniline/CuO nanoparticle composites for use in selective H2S sensors. ACS Appl Nano Mater. 2023;6(19):18413-25. https://doi.org/10.1021/acsanm.3c03732
23. Makarov GN. Laser applications in nanotechnology: nanofabrication using laser ablation and laser nanolithography. Phys Usp. 2013;56(7):643-82. http://dx.doi.org/10.3367/UFNe.0183.201307a.0673
24. Sze SM. Physics of semiconductor devices. 2nd ed. New York: John Wiley and Sons; 1981
25. Zahra S, Syed WAA, Rafiq N, Shah WH, Iqbal Z. On structural, optical, and electrical properties of chromium oxide Cr2O3 thin film for applications. Prot Met Phys Chem Surf. 2021;57(2):321-8. https://doi.org/10.1134/S2070205121010238
26. Hones P, Diserens M, Lévy F. Characterization of sputter-deposited chromium oxide thin films. Surf Coat Technol. 1999;120-121:277-83. https://doi.org/10.1016/S0257-8972(99)00384-9
27. Nguyen TA, Moharana S, Sahu BB, Satpathy SK. Electric and electronic applications of metal oxides. 1st ed. Cambridge (MA): Elsevier; 2025. https://doi.org/10.1016/C2023-0-50311-8
28. Xavier AM, Jacob DI, Surender S, Saravana kumaar MSS, Elangovan P. Structural, optical and electronic properties of copper doped TiO2: combined experimental and DFT study. Inorg Chem Commun. 2022;146:110168. https://doi.org/10.1016/j.inoche.2022.110168
29. Wu J, Luo Y, Qin Z. Composite-modified nano-TiO2 for the degradation of automobile exhaust in tunnels. Constr Build Mater. 2023;408:133805. https://doi.org/10.1016/j.conbuildmat.2023.133805
30. Wang L, Xu S, Yang J, Huang H, Huo Z, Li J. Recent progress in solar-blind photodetectors based on ultrawide bandgap semiconductors. ACS Omega. 2024;9(24):25429-47. https://doi.org/10.1021/acsomega.4c02897
31. Tilley RJD. Defects in solids. Hoboken (NJ): John Wiley & Sons, Inc.; 2008. ISBN: 978-0-470-07794-8. https://doi.org/10.1002/9780470380758
32. Dutta T, Noushin T, Tabassum S, Mishra SK. Road map of semiconductor metal-oxide-based sensors: a review. Sensors. 2023;23(15):6849. https://doi.org/10.3390/s23156849